Ab Initio Calculation and Multiphoton Ionization Studies of Pyrimidine−(Methanol)$_n$ Clusters

Bailin Zhang,* Yong Cai, Xiaolan Mu, Nanquan Lou, and Xiuyan Wang*

State Key Laboratory of Molecular Reaction Dynamics, Dalian Institute of Chemical Physics, Chinese Academy of Sciences, Dalian 116023, P.R. China

Received: July 23, 2001; In Final Form: October 4, 2001

The multiphoton ionization of the hydrogen-bonded clusters $C_4H_4N_2-(CH_3OH)_n$ was studied using a time-of-flight mass spectrometer at the wavelengths of 355 and 532 nm. At both wavelengths, a series of $C_4H_4N_2-(CH_3OH)_nH^+$ ions were obtained. The clusters were also studied by ab initio calculations at B3LYP/6-31G**, MP2/6-31G**, and B3LYP/6-311+G(2df,2p) levels. The equilibrium geometries of both neutral and ionic $C_4H_4N_2-(CH_3OH)_n$ ($n = 1, 2$) clusters and the dissociation channels and dissociaton energies of the ionic clusters are presented. The results show that when $C_4H_4N_2-CH_3OH$ is vertically ionized, $C_4H_4N_2H^+$ and CH_3O are the dominant products via a fast proton-transfer reaction. A high energy barrier makes another channel corresponding to the production of $C_4H_4N_2H^+$ and CH_2OH disfavored. The dominant dissociation products of $C_4H_4N_2-(CH_3OH)_2^+$ should be protonated ions $C_4H_4N_2-(CH_3OH)H^+$. In $C_4H_4N_2-(CH_3OH)H^+$, the proton prefers to link with the N atom of pyrimidine.

I. Introduction

Proton transfer through hydrogen bonding is an important mechanism of many chemical and biological processes.[1−3] It has received a great deal of attention of many theoreticians and experimentalists because of its importance in elucidating various phenomena in nature.[4−6] It has been found that in the ionization processes (such as multiphoton ionization) of many hydrogen-bonded clusters, the predominant products were the protonated ones, and sometimes they were nearly the only ones. These protonated products are suggested to arise from an intracluster proton-transfer reaction accompanying the dissociation processes.[7−9]

Pyrimidine ($C_4H_4N_2$) is a compound of six-membered, nitrogenated aromatic ring, in which exist two different proton-acceptor sites: the ring π cloud and the lone pairs on the heteroatoms. The structural features of the pyrimidine ring are found in a variety of important biological molecules. It is, in particular, the main constituent of nucleotides. Caminati et al.[10] investigated the pyrimidine−water cluster by use of millimeter wave and microwave Fourier transform. The moments of inertia they derived were consistent with a planar (or nearly planar) structure of the cluster in which one hydrogen of the water molecule is bound to the nitrogen of the aromatic ring and the "free" water hydrogen is entgegen to the ring. Matrix isolation FT-IR studies and ab initio calculations[11] suggested the presence of N···H−OH in the pyrimidine−water cluster. As a whole, there is scarce data regarding the pyrimidine−methanol clusters, which are the simplest clusters that can be directly compared with those of pyrimidine−water clusters. The only available result is the hydrogen bonding properties of pyrimidine−methanol cluster studied by Nobeli et al.[12] with distributed multipole analysis (DMA) and intermolecular perturbation theory (IMPT) methods.

In this work, we present ab initio calculations and multiphoton ionization studies of pyrimidine−methanol clusters.

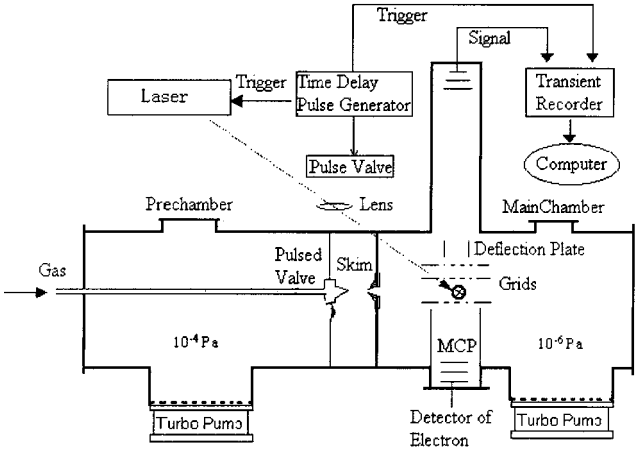

Figure 1. Scheme of the experimental setup.

II. Experimental Section

All experiments were performed on a homemade time-of-flight (TOF) mass spectrometer. A schematic diagram of the TOF mass spectrometer used in the experiments is shown in Figure 1. Pyrimidine- and methanol-mixed clusters were introduced through a 0.29 mm pulsed nozzle into the ionization region located at the main chamber that was separated from the prechamber by a skimmer. The laser beam (Nd: YAG with a pulse width of 10 ns, a maximum output power of about 35mJ for 532 nm and 13mJ for 355 nm per pulse) focused by a quartz lens intersected the cluster beam. Ions formed by the photoionization were accelerated in a double electrostatic field of 0.8 kV in the direction perpendicular to both laser and molecular beams and directed through a 0.8 m long free-field flight tube, which was differentially pumped by two 1500 L/S turbomolecular pumps. The base pressure in the main chamber was maintained at 8.0×10^{-6} Pa and pressure in the prechamber typically raised from 6×10^{-6} Pa to about 8.0×10^{-4} Pa during normal operation. The ions were then detected by a micro-

10.1021/jp012799m CCC: $20.00
Published on Web 11/02/2001

channel plate (MCP) detector connected with a fast preamplifier. The mass spectrum was recorded by a 500 MHz transient recorder (EG&G, Model 9846-500) coupled with a computer. The experiments were operated at 5 Hz and TOF spectra were accumulated from 1024 pulses.

Pyrimidine (Fluka, purum > 98%) and methanol (Shanghai Chemical Industry, 99.9%) were carried by helium (Dalian Chemical Industry, 99.999%) into the ionizer through the pulsed valve. All samples were used without further purification.

III. Computational Details

The program GAUSSIAN98 (Rev. A.9)[13] was used in the computations. For all the molecules and clusters considered in this work, the initial geometries were optimized at the B3LYP density functional method with the 6-31G** standard basis set, and MP2/6-31G** single-point calculations were performed on the optimized structures. Stationary points were confirmed through the calculation of vibrational frequencies, which were also used to evaluate the zero-point vibrational energies. The transition state was verified by frequency and IRC calculations. For the dissociation energy of the neutral $C_4H_4N_2-CH_3OH$ cluster, the basis set superposition error (BSSE) correction was carried out using the counterpoise (CP) method. Since the value of $\langle S^2\rangle = 0.76-0.77$, close to the ideal value 0.75, spin contamination was negligible. To give a comparison, some calculations were also carried out at the B3LYP/6-311+G(2df,-2p) level.

IV. Results and Discussion

A. Mass Spectra. The typical mass spectra of $C_4H_4N_2-(CH_3OH)_n$ clusters at the laser wavelengths of 355 and 532 nm are shown in panels a and b of Figure 2. Both figures exhibit a sequence of protonated ions $C_4H_4N_2-(CH_3OH)_nH^+$, while the relevant unprotonated ions could not be detected. Additionally, a series of protonated methanol cluster ions $(CH_3OH)_nH^+$ can also be seen both at 355 and 532 nm laser. The intensities of $(CH_3OH)_nH^+$ are higher than those of $C_4H_4N_2-(CH_3OH)_nH^+$, which may be the reason that the saturation atmosphere of pyrimidine ($C_4H_4N_2$) is smaller than that of methanol (CH_3OH). Thus, the concentration of CH_3OH is higher than that of $C_4H_4N_2$ in the beam. In Figure 2, the intensity of the protonated cluster ions $C_4H_4N_2-(CH_3OH)_nH^+$ decrease with increasing n, and there are no obvious "magic" numbers to be found.

B. Equilibrium Structures of Neutral and Ionic $C_4H_4N_2-(CH_3OH)_n$ Clusters. Figure 3 depicts the calculated equilibrium structures and parameters of both neutral and ionic $C_4H_4N_2-(CH_3OH)_n$ clusters at the B3LYP/6-31G** level.

As can be seen from Figure 3a, the neutral $C_4H_4N_2-CH_3OH$ cluster forms a bent hydrogen bonding structure N···H−O, and the distance between N and O is 2.867 Å. Both the distance and the shape of N···H−O are similar to those of N···H−O in pyrimidine−water cluster ($C_4H_4N_2-H_2O$).[10] Due to the formation of hydrogen bond N···H−O, the O−H bond is a little longer than that in CH_3OH molecule [R(O−H) of CH_3OH calculated at the B3LYP/6-31G** level is 0.965 Å].

For the ionic $C_4H_4N_2-CH_3OH$ cluster, geometry optimization gives two equilibrium structures: I and II, which are shown in panels b and c of Figure 3, respectively. The bridging H atom of structure I corresponds to H of the hydroxyl group. Structure II is the result of an intracluster reaction in which H in the methyl group of CH_3OH rearranges onto the O atom. From the energies listed in Table 1, it can be seen that structure II is more stable than structure I, which is analogous to the result reported in ref 14.

TABLE 1: Calculated Total Energy (E) and Zero-Point Vibrational Energy (ZPE) for the Pyrimidine, Methanol, and Cluster Species (Unit: hatrees)

species	E (B3LYP)[a]	ZPE (B3LYP)[a]	E (MP2)[b]
CH_3O	−115.0546	0.0368	−114.7094
CH_2OH	−115.0608	0.0375	−114.7241
CH_3OH	−115.7218	0.0505	−115.3769
$CH_3OH-OCH_3$	−230.7891	0.0908	−230.1037
$C_4H_4N_2$	−264.3295	0.0771	−263.5403
$C_4H_4N_2^+$	−263.9997	0.0757	−263.1776
$C_4H_4N_2H^+$	−264.6870	0.0907	−263.8947
$C_4H_4N_2-CH_3OH$	−380.0657	0.1308	−379.0000
$C_4H_4N_2-CH_3OH^+_{ver}$[c]	−379.7298	0.1285	−378.5899
$C_4H_4N_2-CH_3OH^+$ (I)	−379.7705	0.1285	−378.6313
$C_4H_4N_2-CH_3OH^+$ (II)	−379.7758	0.1295	−378.7050
TS (I↔II)	−379.7151	0.1245	−378.6379
$C_4H_4N_2-CH_3OH-H^+$	−380.4466	0.1435	−379.3710
$C_4H_4N_2-(CH_3OH)_2$ (I)	−495.8073	0.1845	−494.4323
$C_4H_4N_2-(CH_3OH)_2$ (II)	−495.8014	0.1844	−494.4283
$C_4H_4N_2-(CH_3OH)_2^+$	−495.5225	0.1814	−494.0399

[a] B3LYP/6-31G**//B3LYP/6-31G** values. [b] MP2/6-31G**//B3LYP/6-31G** values. [c] The subscript ver indicates vertical ionization.

Figure 3b,c shows that the two ionic clusters $C_4H_4N_2-CH_3OH^+$ have nearly linear hydrogen bonding structure. However, being largely different from the neutral, the N−O bond length is shortened, and the bridging H atom is closer to N, which makes the ionic clusters look like $(C_4H_4N_2H\cdots OCH_3)^+$ and $(C_4H_4N_2H\cdots OHCH_2)^+$ but not $(C_4H_4N\cdots HOCH_3)^+$. Namely, both the two ionic structure show obvious "proton transfer" characters. This kind of change of structure is comparable to that of $(CH_3OH)_2^+$, $(H_2O)_2^+$, and $(NH_3)_2^+$.[14] Additionally, the hydrogen bond length R_{N-O} decrease 0.201 Å (ionic structure I) and 0.240 Å (ionic structure II) relative to that of the neutral, respectively, mainly due to a stronger electrostatic interaction in the ions.

Two structures of $C_4H_4N_2-(CH_3OH)_2$ were found in Figure 3e,f. $C_4H_4N_2-(CH_3OH)_2$ (I) has a chain of methanol molecules, which is terminated by π hydrogen bonding to the ortho nitrogen, as seen in the Figure. $C_4H_4N_2-(CH_3OH)_2$ (II) has two analogous hydrogen bonds to that in $C_4H_4N_2-CH_3OH$ cluster. The two methanol molecules are located symmetrically on both sides of the pyrimidine ring, and the two methyl groups of methanol molecules are at the same side of pyrimidine plane. From the energies given in Table 1, it can be known that $C_4H_4N_2-(CH_3OH)_2$ (I) has lower energy than $C_4H_4N_2-(CH_3OH)_2$ (II). Thus, it can be deduced that the stable configuration of $C_4H_4N_2-(CH_3OH)_2$ should be structure I.

The most stable ionic structure of $C_4H_4N_2-(CH_3OH)_2$ was shown in Figure 3g. The ionic structure is largely different from the two neutral structures. The hydrogen bonds N−H···O and O−H···O are nearly linear. The most important geometrical change upon ionization corresponds to the R_{N-O} hydrogen bond length, which decreases 0.279 Å (0.4 Å) relative to the neutral structure e (f), mainly due to a stronger electrostatic interaction in the ion. In the N−H···O bond, the bridging H atom corresponds to the H atom of hydroxyl group of another methanol molecule and is closer to the N atom; namely, it is of a "proton transfer" structure.

The structure of protonated ion $C_4H_4N_2-(CH_3OH)H^+$ is shown in Figure 3h. The pyrimidine and methanol molecules are connected by a bridging atom. Thus, a nearly linear hydrogen bond formed.

C. Dissociation and Proton Transfer Reactions within $C_4H_4N_2-(CH_3OH)_n^+$ Clusters. The calculated energy diagram for the $C_4H_4N_2-CH_3OH$ binary cluster and the energy changes of reactions for $C_4H_4N_2-(CH_3OH)_n$ ($n = 1, 2$) cluster systems are summarized in Figure 4 and Table 2, respectively. Table 2

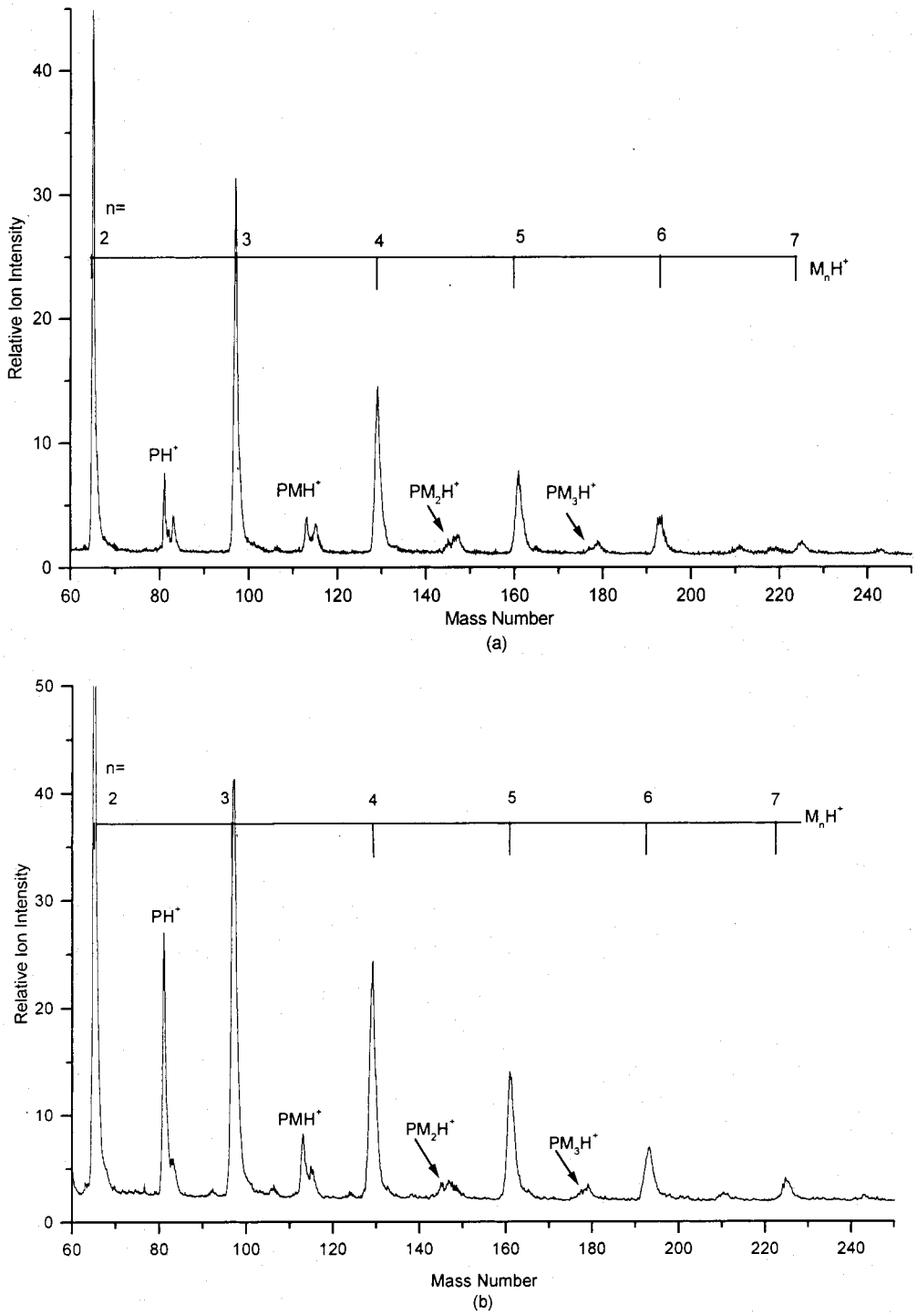

Figure 2. TOF mass spectra of $C_4H_4N_2-(CH_3OH)_n$ (a) obtained at 355 and (b) 532 nm laser. M_nH^+, $(CH_3OH)_nH^+$; PM_nH^+, $C_4H_4N_2-(CH_3OH)_nH^+$.

also lists the results obtained by other techniques for comparison. It can be seen that the calculation results obtained at present level of theory are in agreement with other theoretical and experimental results.[12,16,17] From the dissociation energy after BSSE correction of the $C_4H_4N_2-CH_3OH$ cluster given in Table 2, it can be known that the BSSE error is not significant in this basis set.

In Figure 4, $(C_4H_4N_2-CH_3OH)^+_{ver}$ indicates vertically ionized $C_4H_4N_2-CH_3OH$ from the optimized ground state of neutral $C_4H_4N_2-CH_3OH$ cluster and is set to be zero. From Figure 4, it can be known that $(C_4H_4N_2-CH_3OH)^+_{ver}$ has a higher energy than that necessary for the dissociation to produce $C_4H_4N_2H^+ + CH_3O$ or $C_4H_4N_2H^+ + CH_2OH$ but not enough for the dissociation to produce $C_4H_4N_2^+ + CH_3OH$. Thus, it can be expected that for $C_4H_4N_2-CH_3OH$ or larger clusters, the measured ions after ionization should be a sequence of protonated products, which agrees with the experimental results in Figure 2 well. The channel corresponding to produce $C_4H_4N_2H^+ + CH_2OH$ seems to need less energy, but the dissociation process should follow an intracluster rearrangement reaction $[C_4H_4N_2-CH_3OH^+$ (I) $\rightarrow C_4H_4N_2-CH_3OH^+$ (II)]. Namely, H in the methyl group moves onto the O atom. At B3LYP/6-31G** level, the calculated configuration of the transition state (TS) (confirmed by frequency and IRC calculations) is shown in Figure 3d. As shown in Figure 4, an energy barrier of ~32 kcal mol $^{-1}$ makes the process less favored than that producing

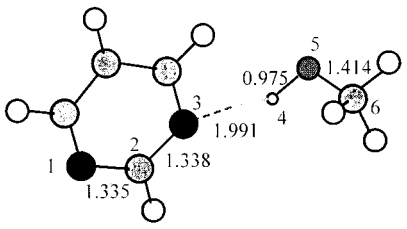

(a) $C_4H_4N_2$-CH_3OH

∠N1C2N3=126.8; ∠C2N3H4=144.5; ∠H4O5C6=107.7; ∠O5H4N3C2=-171.8; ∠C6O5H4N3=103.0; ∠N3H4O5=148.4.

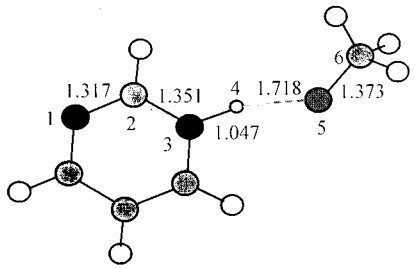

(b) $C_4H_4N_2$-CH_3OH^+ (I)

∠N1C2N3=123.0; ∠C2N3H4=121.1; ∠N3H4O5=160.1; ∠H4O5C6=133.6; ∠O5H4N3C2=-179.9; ∠C6O5H4N3=-178.7.

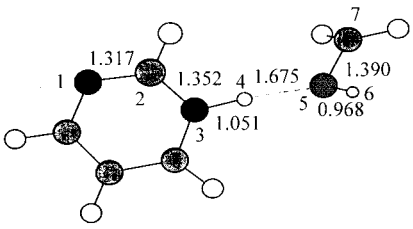

(c) $C_4H_4N_2$-CH_3OH^+ (II)

∠N1C2N3=123.0; ∠C2N3H4=119.5; ∠N3H4O5=176.1; ∠H4O5C7=120.6; ∠H6O5C7=110.1; ∠O5H4N3C2=-144.5; ∠C7O5H4N3=79.7; ∠H6O5H4N3=-133.9.

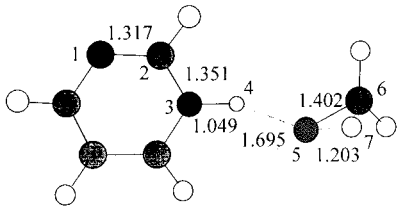

(d) TS (I↔II)

∠C2N3H4=121.3; ∠N3H4O5=158.0; ∠H4O5C6=133.7; ∠O5H4N3C2=179.8; ∠C6O5H4N3=148.3; ∠H7O5H4N3=-133.8.

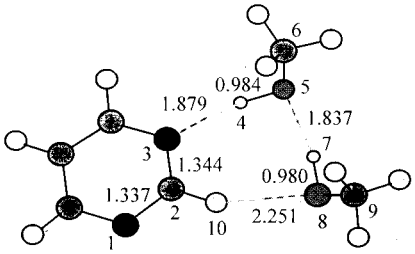

(e) $C_4H_4N_2$-$(CH_3OH)_2$ (I)

∠N1C2N3=125.9; ∠C2N3H4=113.4; ∠N3H4O5=166.7; ∠H4O5C6=108.0; ∠O5H7O8=163.9; ∠O8H10C2=152.9; ∠O5H4N3C2=-19.8; ∠O8H7O5H4=-20.4.

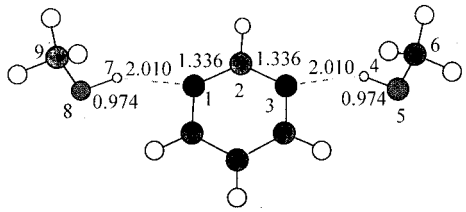

(f) $C_4H_4N_2$-$(CH_3OH)_2$

∠C2N3H4=∠C2N1H7=144.9; ∠N3H4O5=∠N1H7O8=147.0; ∠O5H4N3C2=∠O8H7N1C2=-173.1; ∠C6O5H4N3=C9O8H7N1=-105.0.

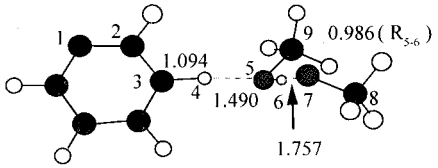

(g) $C_4H_4N_2$-$(CH_3OH)_2^+$

∠C2N3H4=120.3; ∠N3H4O5=174.1; ∠O5H6O7=171.4; ∠O5H4N3C2=174.3; ∠O7H6O5H4=-29.2; ∠C8O7O5C9=-68.5.

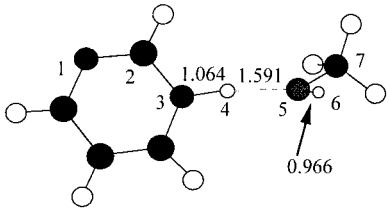

(h) $C_4H_4N_2$-CH_3OH-H^+

∠O5H4N3=171.7; ∠O5H4N3C2=-178.1; ∠C7O5H4N3=-178.1.

Figure 3. Geometries of pyrimidine−methanol clusters ($C_4H_4N_2$−$CH_3OH)_n$) calculated with the B3LYP/6-31G** method.

$C_4H_4N_2H^+ + CH_3O$. This conclusion is consistent with experimental results that show that both $D^+(CH_3OH)_n$ and $H^+(CD_3OH)_n$ are formed in the ionization of CD_3OH cluster; however, $D^+(CD_3OH)_n$ has less abundance than $H^+(CD_3OH)_n$.[18]

The analysis of the molecular orbits shows that the highest occupied molecular orbit (HOMO) of the neural cluster is located primarily on the 2p and 3p orbits of O atom, which means the removal of an electron occurs mainly from the O atom. This also can be verified by the Mulliken population of atomic charges of the neutral and vertically ionized clusters. On vertical ionization associated with $C_4H_4N_2$−CH_3OH^+ (I), the atomic charge of O increases from −0.6 to −0.3, whereas the other atoms change little. Though the methanol has a higher ionization potential (IP) than pyrimidine,[16,19,20] the IP values do not offer conclusive indications of the site at which initial excitation or ionization will occur. For example, in the studies of $Ar_n(CH_3OH)_m$, though the IP value of Ar is higher than that of CH_3OH, Garvey et al.[21] conclude that the ionization of the methanol molecule is first being mediated by the Ar 4s excited state; namely, intracluster penning ionization occurred. Additionally, the IP value of $C_4H_4N_2$−CH_3OH calculated in this work of ∼183.8 kcal mol^{-1} is obviously smaller than the IP of

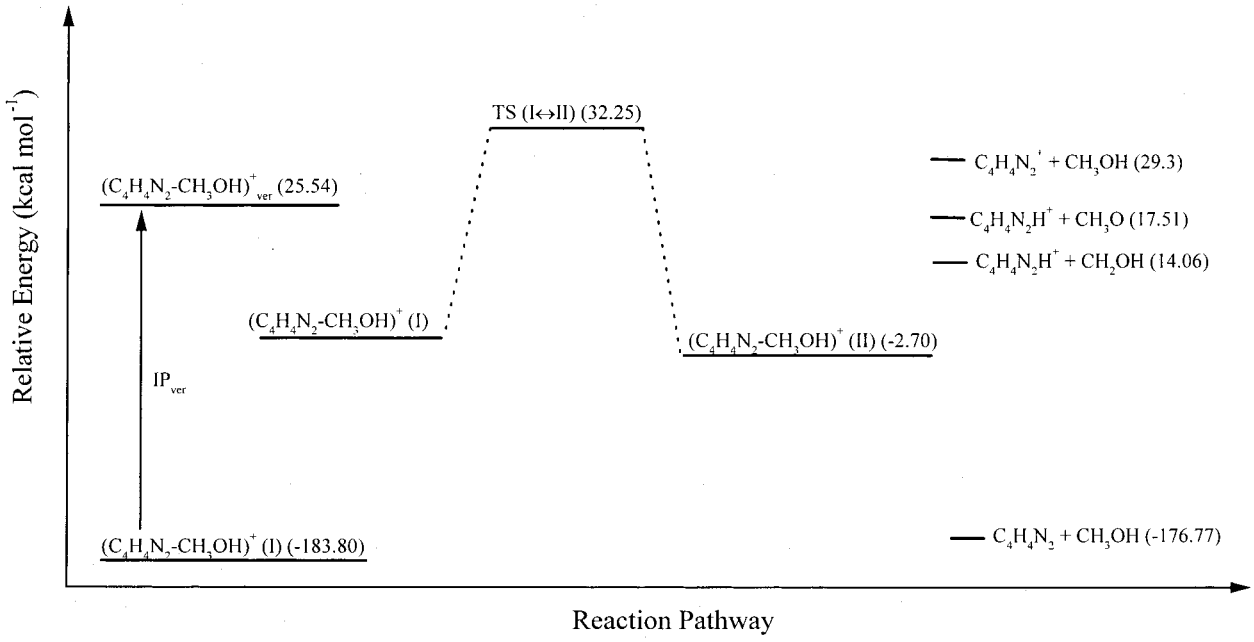

Figure 4. Schematic energy diagram for the intracluster dissociation and proton transfer reactions of ionic pyrimidine−methanol clusters. The energies of all species were obtained at the B3LYP/6-31G**//B3LYP/6-31G** level with zero-point vibrational energy corrections. The relative energies in parentheses are relative to the energy of $(C_4H_4N_2-CH_3OH)^+$ (I), which is set to be zero.

TABLE 2: Summary of the Reaction Energies for Pyrimidine−Methanol Cluster Systems (kcal mol^{-1})[a]

	reaction		energy	other results
1	$C_4H_4N_2$	$\rightarrow C_4H_4N_2^+$	IP = 206.07	209.85[c]
2	$C_4H_4N_2 + H^+$	$\rightarrow C_4H_4N_2H^+$	PA = 215.80	211.74[d]
3	$C_4H_4N_2-CH_3OH$	$\rightarrow C_4H_4N_2 + CH_3OH$	D_e = 9.0 (7.87$_{BSSE}$)	6.70;[e] 5.88[f]
			D_0 = 7.03 (6.5$_{BSSE}$)[g]	
4		$\rightarrow C_4H_4N_2-CH_3OH^+$ (I)	IP = 183.80	
5		$\rightarrow C_4H_4N_2-CH_3OH^+_{ver}$[b]	IP_{ver} = 209.34	
6		$\rightarrow C_4H_4N_2-CH_3OH^+$ (II)	IP = 181.10	
7	$C_4H_4N_2-CH_3OH + H^+$	$\rightarrow C_4H_4N_2-CH_3OH-H^+$	PA = 231.05	
8	$C_4H_4N_2-CH_3OH^+$ (I)	$\rightarrow C_4H_4N_2^+ + CH_3OH$	D_0 = 29.30	
9		$\rightarrow C_4H_4N_2H^+ + CH_3O$	D_0 = 17.51	
10	$C_4H_4N_2-CH_3OH^+$ (II)	$\rightarrow C_4H_4N_2H^+ + CH_2OH$	D_0 = 16.75	
11	$C_4H_4N_2-CH_3OH^+$ (I)	$\rightarrow$ TS (I↔II)	ΔE = 32.25	
12	$C_4H_4N_2-CH_3OH^+$ (II)	$\rightarrow$ TS (I↔II)	ΔE = 34.95	
13	$C_4H_4N_2-(CH_3OH)_2$ (I)	$\rightarrow C_4H_4N_2 + 2CH_3OH$	D_0 = 17.44	
14	$C_4H_4N_2-(CH_3OH)_2$ (II)	$\rightarrow C_4H_4N_2 + 2CH_3OH$	D_0 = 13.81	
15	$C_4H_4N_2-(CH_3OH)_2$ (I)	$\rightarrow C_4H_4N_2-(CH_3OH)_2+$	IP = 176.77	
16	$C_4H_4N_2-(CH_3OH)_2+$	$\rightarrow C_4H_4N_2^+ + 2CH_3OH$	D_0 = 46.75	
17		$\rightarrow C_4H_4N_2-CH_3OH-H^+ + CH_3O$	D_0 = 12.68	
18		$\rightarrow C_4H_4N_2H^+ + CH_3OH-OCH_3$	D_0 = 29.18	

[a] B3LYP/6-31G**//B3LYP/6-31G** + ZPE values. [b] The subscript ver indicates vertical ionization. [c] Ref 16. [d] Ref 17. [e] DMA (distributed multipole analysis) + 6-exp value (ref 12). [f] IMPT (intermolecular perturbation theory) value (ref 12). [g] BSSE indicates BSSE error corrected.

pyrimidine, and the IP value (176.77 kcal mol^{-1}) of $C_4H_4N_2-(CH_3OH)_2$ is even smaller than that of $C_4H_4N_2$. Analogous result that the formation of a cluster may cause the IP value of a monomer to be red-shifted was also reported.[22] Thus it is possible that the methanol in the $C_4H_4N_2-CH_3OH$ can be ionized or excited first. The Mulliken population of the total atomic charge of CH_3OH in $C_4H_4N_2-CH_3OH$, $C_4H_4N_2-CH_3OH^+_{ver}$, and $C_4H_4N_2-CH_3OH^+$ (I) is −0.03, 0.48, and 0.10, respectively, which may mean that intracluster charge-transfer process may take place after the vertical ionization.

From reactions in Table 2, it can be known that both the $C_4H_4N_2-CH_3OH^+$ (I) and $C_4H_4N_2-(CH_3OH)_2^+$ can dissociate to produce protonated ion $C_4H_4N_2H^+$ through reactions 9 and 18, respectively; however, reaction 9 is energetically favored by 12.3 kcal mol^{-1}. Thus, it can be deduced that $C_4H_4N_2H^+$ is mainly the dissociation product of $C_4H_4N_2-CH_3OH^+$ (I). As shown in Table 2, it can also be known that the dissociation of $C_4H_4N_2-(CH_3OH)_2^+$ can produce unprotonated and protonated ions. But the channel corresponding to produce $C_4H_4N_2-(CH_3OH)H^+ + CH_3O$ is the best energy favored. According to above discussion, the protonated clusters $C_4H_4N_2-(CH_3OH)_nH^+$ can be suggested to be produced by the following ionization-intracluster proton transfer-dissociation reactions:

$$C_4H_4N_2-(CH_3OH)_m + k h\nu \rightarrow C_4H_4N_2-(CH_3OH)_m^+ + e^- \rightarrow C_4H_4N_2-(CH_3OH)_nH^+ + (CH_3OH)_{m-n-1} + CH_3O + e^-$$

To elucidate the reaction mechanism of intracluster proton transfer after cluster photoionization, an ab initio calculation of simplified reaction path potential was performed on the optimized structures of $C_4H_4N_2-CH_3OH$ and $C_4H_4N_2-CH_3OH^+$ (I) with B3LYP/6-31G** and B3LYP/6-311+G(2df,2p) methods. As shown in Figure 3a,, the hydrogen bond N···H−O is obviously bent. Analogous to the model[23−25] for bent hydrogen systems, during the calculations, the hydrogen bond length (the sum of the actual N−H distance and H−O distance)

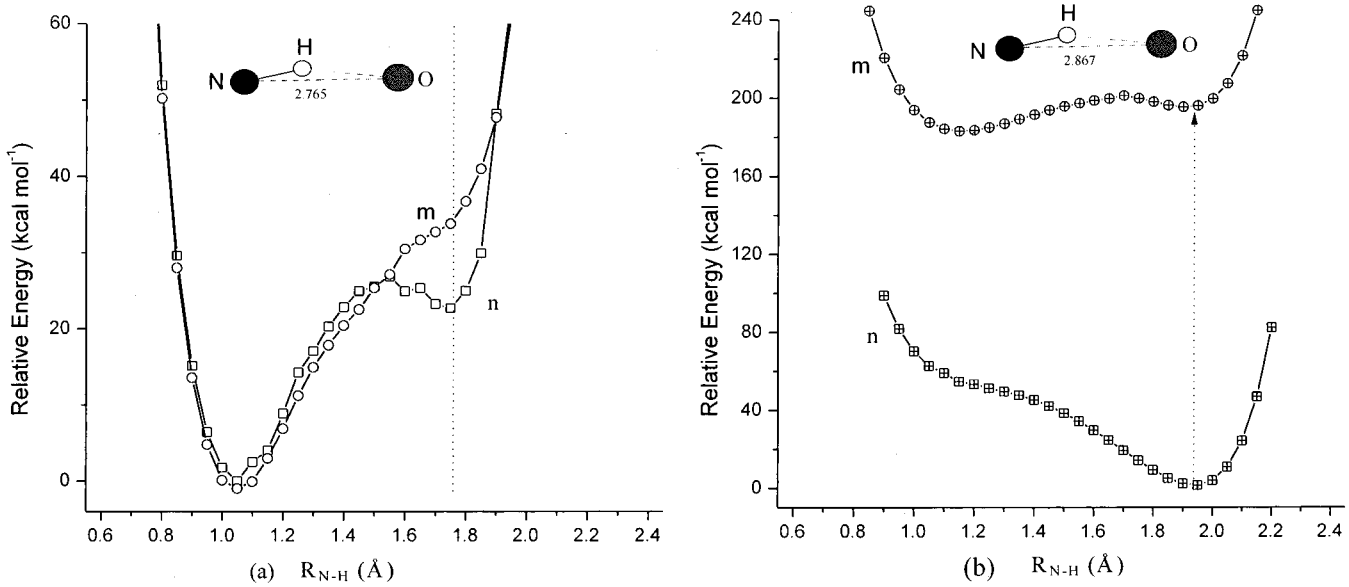

Figure 5. Potential energy curves of ionic cluster $(C_4H_4N_2\cdots HOCH_3)+$ (I) and neutral cluster $C_4H_4N_2-CH_3OH$ at different calculation levels. R_{N-H} is the distance between the N and O atom. (a) Potential energy curves m and n of the ionic cluster are calculated with the B3LYP/6-311+G-(2df,2p) and B3LYP/6-31G** levels, respectively. (b) Potential energy curve n and vertical ionization potential curve m of the neutral cluster are calculated with the B3LYP/6-31G** level.

is fixed at the optimized value. Additionally, the optimized distance of N−O was also fixed to be the optimized value 2.765 Å (ionic) and 2.866 Å (neutral). Relative to that of the C, N, O heavy atoms, the movement of the lighter bridging H atom should be much faster. Thus, the heavy atoms could be considered to be stationary. For the other H atoms in methyl and $C_4H_4N_2$, their effects on the bridging hydrogen were neglected. From the calculation configuration, it can be seen that these atoms vary little. According to the above hypothesis, the potential energy of $(C_4H_4N_2-CH_3OH)^+$ (I) cluster was calculated with B3LYP/6-31G** and B3LYP/6-311+G(2df,-2p) levels, with the bridging hydrogen moving across toward the oxygen in steps (step size is 0.05 Å). The potential of neutral $C_4H_4N_2-CH_3OH$ and the vertical ionization potential were calculated only by using of B3LYP/6-31G** level. The potential energy curves of ionic and neutral clusters are shown in Figure 5. It shows that for the neutral cluster [as shown in Figure 5b (curve n)], the bridging H atom tends to be closer to the O atom than the N atom. After vertical ionization, the bridging H atom prefers to move to N atom [as shown in Figure 5b (curve m)]. However, the ionic cluster (Figure 5a) is largely different, and two potential wells exist at the 6−31** level, which correspond to $(C_4H_4N_2\cdots HOCH_3)^+$ and $(C_4H_4N_2H^+\cdots OCH_3)^+$. The transfer of the proton across to the nitrogen is favored by ∼20 kcal mol $^{-1}$. This transfer is blocked by a small barrier of only ∼5 kcal mol^{-1}. At the B3LYP/6-311+G(2df,2p) level, the minimum associated with $(C_4H_4N_2\cdots HOCH_3)^+$ disappears. Thus, it is expected that after the vertical ionization, the intracluster proton-transfer process from $(C_4H_4N_2\cdots HOCH_3)^+$ to $(C_4H_4N_2H\cdots OCH_3)^+$ should occur quickly. From the energy diagram shown in Figure 4, it can be known when $C_4H_4N_2-CH_3OH$ is vertically ionized, the surplus energy is enough to make the ionic cluster dissociate into $C_4H_4N_2H^+$ and CH_3O. Thus, the protonated cluster ions should be the dominant product, which can be verified by the experimental results in Figure 3.

D. Position of the Proton in $C_4H_4N_2-(CH_3OH)H^+$ Clusters. To determine if the proton in cluster $C_4H_4N_2-(CH_3OH)-H^+$ prefers to link with the N atom of $C_4H_4N_2$ or the O atom of CH_3OH, analogous potential energy calculations to $C_4H_4N_2-CH_3OH^+$ for $C_4H_4N_2-(CH_3OH)H^+$ were carried out with the SCF/6-31G**, MP2/6-31G**, and B3LYP/6-31G** methods. The obtained energy curve is shown in Figure 6. There exist two potential wells at SCF/6-31G** level, which correspond to $(C_4H_4N_2\cdots HOHCH_3)^+$ and $(C_4H_4N_2H\cdots OHCH_3)^+$. At the B3LYP/6-31G** and MP2/6-31G** levels, the well associated with $(C_4H_4N_2\cdots HOHCH_3)^+$ disappears completely. The study[12] of hydrogen bonds to nitrogen and oxygen atoms in aromatic heterocyclic rings has shown that nitrogen is a significantly better proton acceptor than oxygen. Böhm et al.[26] also found a dramatically larger amount of hydrogen bonds to nitrogen acceptors than to oxygen when the N or O atom is bonded to at least one sp^2 hybridized atom. Additionally, the proton affinity (PA) of $C_4H_4N_2$ is higher than that of CH_3OH[17] [PA($C_4H_4N_2$) = 211.7 kcal mol $^{-1}$; PA(CH_3OH) =165.2 kcal mol $^{-1}$]. Thus, it is reasonable that the proton prefers to link with the N atom of $C_4H_4N_2$.

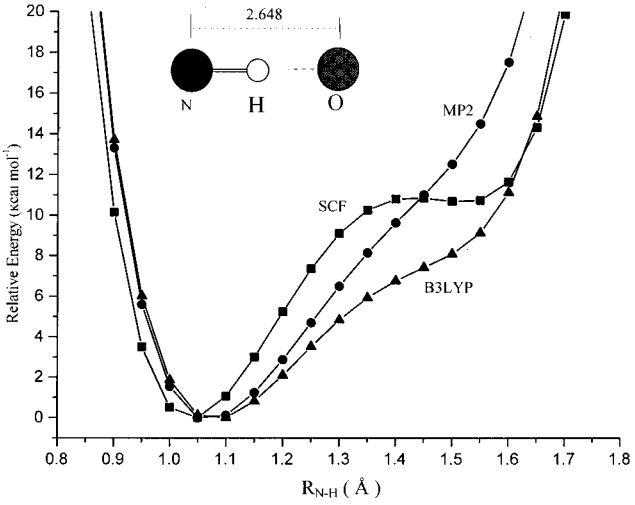

Figure 6. Potential energy curve of protonated ion $(C_4H_4N_2\cdots HOHCH_3)^+$ calculated with the SCF/6-31G**, MP2/6-31G**, and B3LYP/6-31G** levels. R_{N-H} is the distance between the N and H atoms. R_{N-O} is fixed at the optimized value: 2.648 Å.

V. Conclusion

The laser photoionization of the hydrogen-bonded cluster $C_4H_4N_2-(CH_3OH)_n$ was studied with a time-of-flight mass spectrometer at the wavelengths of 355 and 532 nm. The results show that, at both wavelengths, a series of $C_4H_4N_2-(CH_3OH)_nH^+$ were obtained. Ab initio calculations also show when $C_4H_4N_2-CH_3OH$ is vertically ionized, the dissociation channel that produces $C_4H_4N_2H^+ + CH_3O$ is the dominant channel through a fast intracluster proton-transfer reaction. For another channel corresponding to produce $C_4H_4N_2H^+ + CH_2OH$, which follows an intracluster rearrangement reaction, a high energy barrier makes it less favored. The dominant dissociation products of $C_4H_4N_2-(CH_3OH)_2^+$ should be protonated ions $C_4H_4N_2-(CH_3OH)H^+$. In $C_4H_4N_2-(CH_3OH)H^+$, the proton prefers to link with the N atom of pyrimidine.

Acknowledgment. This work was supported by the NK-BRSF and NSCF (No. 20073044).

References and Notes

(1) Caldin, E., Gold, V., Eds. In *Proton-Transfer Reaction*; Wiley: New York, 1975, and references therein.

(2) Mitchell P. *Annu. Rev. Biochem*. **1977**, *46*, 996.

(3) Stoeckenius, W.; Bogomolni, R. A. *Annu. Rev. Biochem*. **1982**, *53*, 587, and references therein.

(4) Tzeng, W. B.; Wei, S.; Castleman, A. W., Jr. *Chem. Phys. Lett*. **1990**, *168*, 30.

(5) Devault D. *Quantum Mechanical Tunneling in Biological Systems*; Cambridge University Press: London, 1984.

(6) Xia, P.; Hall, M. T.; Furlani, R.; Garvey, J. F. *J. Phys. Chem*. **1996**, *100*, 12235.

(7) Wei, S.; Purnell, J.; Buzza, S. A.; Stanley, R. J.; Castleman, A. W., Jr. *J. Chem. Phys*. **1993**, *99*, 755.

(8) Castleman, A. W., Jr.; Wei, S. *Annu. Rev. Phys. Chem*. **1994**, *45*, 685.

(9) Berstein, E. R. *Annu. Rev. Phys. Chem*. **1995**, *46*, 197.

(10) Melandri, S.; Sanz, M. E.; Caminati, W.; Favero, P. G.; Kisiel, Z. *J. Am. Chem. Soc*. **1998**, *120*, 11504.

(11) Destexhe, A.; Smets, J.; Adamowicz, L.; Maes, G. *J. Phys. Chem*. **1994**, *98*, 1506.

(12) Nobeli, I.; Price, S. L.; Lommerse, J. P. M.; Taylor, R. *J. Comput. Chem*. **1997**, *18* (16), 2060.

(13) Frisch, M. J.; Trucks, G. W.; Schlegel, H. B.; Scuseria, G. E.; Robb, M. A.; Cheeseman, J. R.; Zakrzewski, V. G.; Montgomery, J. A., Jr.; Stratmann, R. E.; Burant, J. C.; Dapprich, S.; Millam, J. M.; Daniels, A. D.; Kudin, K. N.; Strain, M. C.; Farkas, O.; Tomasi, J.; Barone, V.; Cossi, M.; Cammi, R.; Mennucci, B.; Pomelli, C.; Adamo, C.; Clifford, S.; Ochterski, J.; Petersson, G. A.; Ayala, P. Y.; Cui, Q.; Morokuma, K.; Malick, D. K.; Rabuck, A. D.; Raghavachari, K.; Foresman, J. B.; Cioslowski, J.; Ortiz, J. V.; Stefanov, B. B.; Liu, G.; Liashenko, A.; Piskorz, P.; Komaromi, I.; Gomperts, R.; Martin, R. L.; Fox, D. J.; Keith, T.; Al-Laham, M. A.; Peng, C. Y.; Nanayakkara, A.; Gonzalez, C.; Challacombe, M.; Gill, P. M. W.; Johnson, B. G.; Chen, W.; Wong, M. W.; Andres, J. L.; Head-Gordon, M.; Replogle, E. S.; Pople, J. A. *Gaussian 98*, revision A.9; Gaussian, Inc.: Pittsburgh, PA, 1998.

(14) Lee, S. Y.; Shin, D. N.; Cho, S. G.; Jung, K.-H.; Jung, K. W. *J. Mass. Spectrom*. **1995**, *30*, 969.

(15) Tomoda, S.; Kimura, K. *Vacuum Ultraviolet Photoionization and Photodissociation of Molecules and Clusters*; World Scientific: Singapore, 1991; p 101.

(16) Piancastelli, M. N.; Keller, P. R.; Taylor, J. W.; Grimm, F. A.; Carlson, T. A. *J. Am. Chem. Soc*. **1983**, *105*, 4235.

(17) Hunter, E. P.; Lias, S. G. *J. Phys. Chem. Ref. Data* **1998**, *27*, 3, 413.

(18) El-Shall, M. S.; Marks, C.; Sieck, L. W.; Meat-Ner(Mautner), M. *J. Phys. Chem*. **1992**, *96*, 2045.

(19) Tao, W.; Klemm, R. B.; Nesbitt, F. L.;. Stief, J. L. *J. Phys. Chem*. **1992**, *96*, 104.

(20) Yencha, A. J.; El-Sayed, M. A. *J. Chem. Phys*. **1968**, *48*, 3469.

(21) Vaidyanathan, G.; Coolbaugh, M. T.; Peifer, W. R. and Garvey, F. J. *J. Chem. Phys*. **1991**, *94*, 1850.

(22) Li, Y.; Wang, X. Y.; Zhang, X. G.; Li, L. B.; Lou, N. Q.; Sheng, L. S.; Zhang, Y. W. *Acta Phys.-Chim. Sin*. **1997**, *13*, 322.

(23) Maulton W. G.; Kromhout, R. A. *J. Chem. Phys*. **1956**, *25*, 34.

(24) Maulton, W. G.; Kromhout, R. A. *J. Chem. Phys*. **1955**, *23*, 1673.

(25) Schroder, R.; Lippincott, E. R. *J. Phys. Chem*. **1957**, *61*, 921.

(26) Böhm, H. J.; Brode, S.; Hesse, U.; Klebe, G. *Eur. J*. **1996**, *2*, 1509.